

EFFECT OF SUBSTRATE TEMPERATURE AND DEPOSITION PROFILE ON EVAPORATED Cu(InGa)Se₂ FILMS AND DEVICES

William N. Shafarman and Jie Zhu

Institute of Energy Conversion
University of Delaware, Newark, DE 19716 USA

Abstract

This paper addresses the effect of substrate temperature (T_{ss}) and deposition profile for Cu(InGa)Se₂ films deposited by multisource elemental evaporation on film structure and solar cell performance. Different temporal Cu flux profiles are utilized to give either a graded deposition incorporating a Cu-rich growth step, with $[Cu] > [In]+[Ga]$, before achieving the final film composition with $[Cu] < [In]+[Ga]$, or a uniform deposition with $[Cu] < [In]+[Ga]$ throughout. The Cu(InGa)Se₂ morphology, including quantitative analysis of the grain size distributions, and the performance of completed solar cells are compared at $T_{ss} = 400$ and 550°C . The higher T_{ss} gives larger grains and better device performance with the best devices obtained in this work having efficiency = 16.4% for 550°C and 14.1% for 400°C . At 550°C , Cu-rich film growth gives bigger grains than a uniform flux process, but there is no difference in the device performance. With $T_{ss} = 400^{\circ}\text{C}$, there is no significant difference in the grain size with the different flux profiles, but the Cu-rich growth is needed for improved devices.

Keywords: Cu(InGa)Se₂, solar cells, substrate temperature, grain size, morphology.

Introduction

For solar cells based on thin film Cu(InGa)Se₂ to become a commercially viable technology, manufacturing costs must be reduced. One means to accomplish this is by reducing the substrate temperature at which the Cu(InGa)Se₂ layer is deposited. Soda lime glass is typically used as the substrate for high efficiency Cu(InGa)Se₂ solar cells, but it deforms at the temperatures used for the highest efficiency devices, $550 - 600^{\circ}\text{C}$. A substrate temperature (T_{ss}) less than 480°C is needed to remain below the strain point of soda lime glass. With even lower T_{ss} , alternative substrate materials, like a flexible polymer, could be utilized. In addition, lower T_{ss} can allow faster heat-up and cool-down time and decrease the heat load and thermal stress on the entire deposition system.

This paper will address material and device issues related to reducing T_{SS} from 550°C to 400°C for the deposition of $\text{Cu}(\text{InGa})\text{Se}_2$ by physical vapor deposition using multisource elemental evaporation. Deposition of $\text{Cu}(\text{InGa})\text{Se}_2$ by multisource evaporation typically is done with a process which incorporates a Cu-rich growth step, i.e. deposition with the Cu molar flux greater than the sum of the In and Ga fluxes [1]. With $[\text{Cu}] > [\text{In}] + [\text{Ga}]$, the growing film contains a mixture of $\text{Cu}(\text{InGa})\text{Se}_2$ and Cu_xSe_y , where the specific Cu_xSe_y phase may depend on the temperature [2]. This is then followed by a Cu-deficient growth step so that the final film has the desired composition range with $\text{Cu}/(\text{In}+\text{Ga}) < 1$. This process was found to have an effect on both the film morphology and device performance [1]. We have previously shown that, using a deposition with a Cu-rich growth step and varying T_{SS} from 600°C down to 350°C, the $\text{Cu}(\text{InGa})\text{Se}_2$ grain size decreases over the entire range of T_{SS} and the device efficiency decreases slowly for 550 T_{SS} 400°C [3].

In this work, the effect of substrate temperature and growth process on grain size, morphology and device performance are quantitatively evaluated. The objective is to develop a process for improved device performance with $T_{SS} = 400^\circ\text{C}$. The grain size and morphology, as well as the solar cell device performance, for $\text{Cu}(\text{InGa})\text{Se}_2$ films deposited at 550 or 400°C are compared for different temporal flux profiles during the deposition to determine the effect of a Cu-rich growth step. Specifically, we will compare depositions with a uniform flux, i.e. no Cu-rich growth to depositions with a Cu-rich flux at the beginning of the deposition or a Cu-rich flux in the middle of the deposition. This will distinguish if the effects of Cu-rich growth specifically require the presence of the Cu_xSe_y phase during the initial nucleation of the film on the glass/Mo substrate.

Experimental Procedure

$\text{Cu}(\text{InGa})\text{Se}_2$ films were deposited by thermal evaporation from independently controlled elemental sources for the Cu, In, Ga, and Se. Three temporal deposition flux profiles were used to give depositions with: (1) uniform fluxes so that the films composition was never Cu-rich, (2) Cu-rich flux, $\text{Cu}/(\text{In}+\text{Ga}) > 1$, at the beginning of the run followed by only In, Ga, and Se fluxes to give the desired Cu-deficient final composition, and (3) Cu-rich flux in the middle of the run. These are shown schematically in Fig. 1. The In, Ga, and Se fluxes were kept constant throughout each deposition, so there were no gradients in Ga content or bandgap, and were the same for each flux profile. The differences in the depositions, then, were only in the Cu fluxes. These three flux profiles were done at $T_{SS} = 550$ and 400°C. The deposition time for all films was 44 min. and the final film thicknesses were 2.5 – 3 μm .

All films used for morphological characterization and devices had a final composition, measured by energy dispersive x-ray spectroscopy (EDS), with $\text{Cu}/(\text{In}+\text{Ga}) = 0.8 - 0.9$ and $\text{Cu}/(\text{In}+\text{Ga}) 0.3$. This gives a bandgap of $E_G = 1.2$ eV. Other film characterization included Auger electron spectroscopy (AES) depth profiles, performed at National Renewable Energy Laboratory (NREL), and x-ray diffraction (XRD).

Scanning electron microscopy (SEM) and atomic force microscopy (AFM) were used to characterize the $\text{Cu}(\text{InGa})\text{Se}_2$ morphology and grain size. Tapping mode AFM images, taken on a Digital Instruments Dimension 3100 Scanning Probe Microscope were specifically used to enable the lateral grain size distribution to be quantitatively determined. In some cases, the

Cu(InGa)Se₂ films were first etched in a 2 wt% bromine in methanol solution for 15 sec. to reveal grain boundaries.

All Cu(InGa)Se₂ films were deposited on soda lime glass substrates with a 1 μm thick sputtered Mo layer. Devices were completed by the chemical bath deposition of ~ 30 nm CdS followed by rf sputtered ZnO:Al with thickness 0.5 μm and sheet resistance 20 /sq. An evaporated Ni/Al grid was deposited and cell areas were delineated by mechanical scribing to give area = 0.5 cm². Details of the deposition and cell fabrication are given in [4]. Devices were characterized by current-voltage (J-V) measurements with the sample at 25°C under 100 mW/cm² AM1.5 illumination.

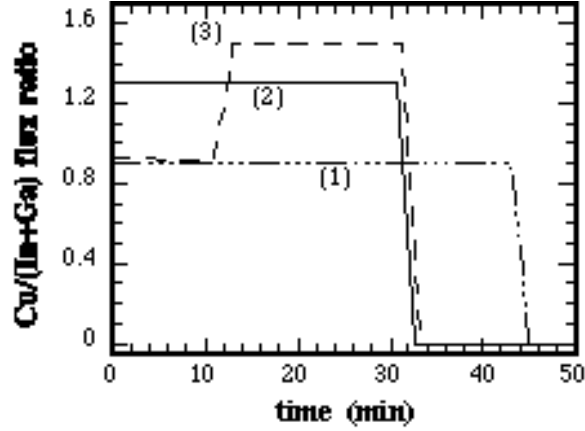


Fig. 1. Schematic representation of three temporal flux profiles defined in the text.

Results

Grain size and composition

SEM cross-sectional micrographs of films grown with the three profiles and two temperatures are shown in Fig. 2. The films grown at $T_{SS} = 550^{\circ}\text{C}$ all have larger grains than those grown at 400°C . At the lower temperature, the uniform flux process appears to give more columnar grains and a smoother surface. There are no apparent differences between films grown with the Cu-rich flux at either the beginning or middle of the deposition.

AFM images of the top surface were used to determine the lateral grain size. This is shown in Fig. 3 for the films grown with a Cu-rich flux at the beginning at each temperature. Again, the higher T_{SS} clearly gives larger grains, while the lower T_{SS} gives a more faceted morphology. To quantify the grain size, a map of the grain boundaries was made from these images as shown in Fig. 4. This map was then digitized and National Institute of Health (NIH) Image software was used to determine the grain sizes. The grain size statistics were collected for 3 randomly selected $10\ \mu\text{m} \times 10\ \mu\text{m}$ areas on each sample. The resulting grain sizes were found to conform to a log-normal distribution which is described by:

$$f(\ln A) = \frac{1}{(\ln A)\sqrt{2}} \exp - \frac{(\ln A - \ln \bar{A})^2}{2 (\ln A)^2} \quad (1)$$

where A is the grain area, \bar{A} is the mean area, and σ is the standard deviation. This distribution is commonly used to describe normal grain size in polycrystalline materials [5].

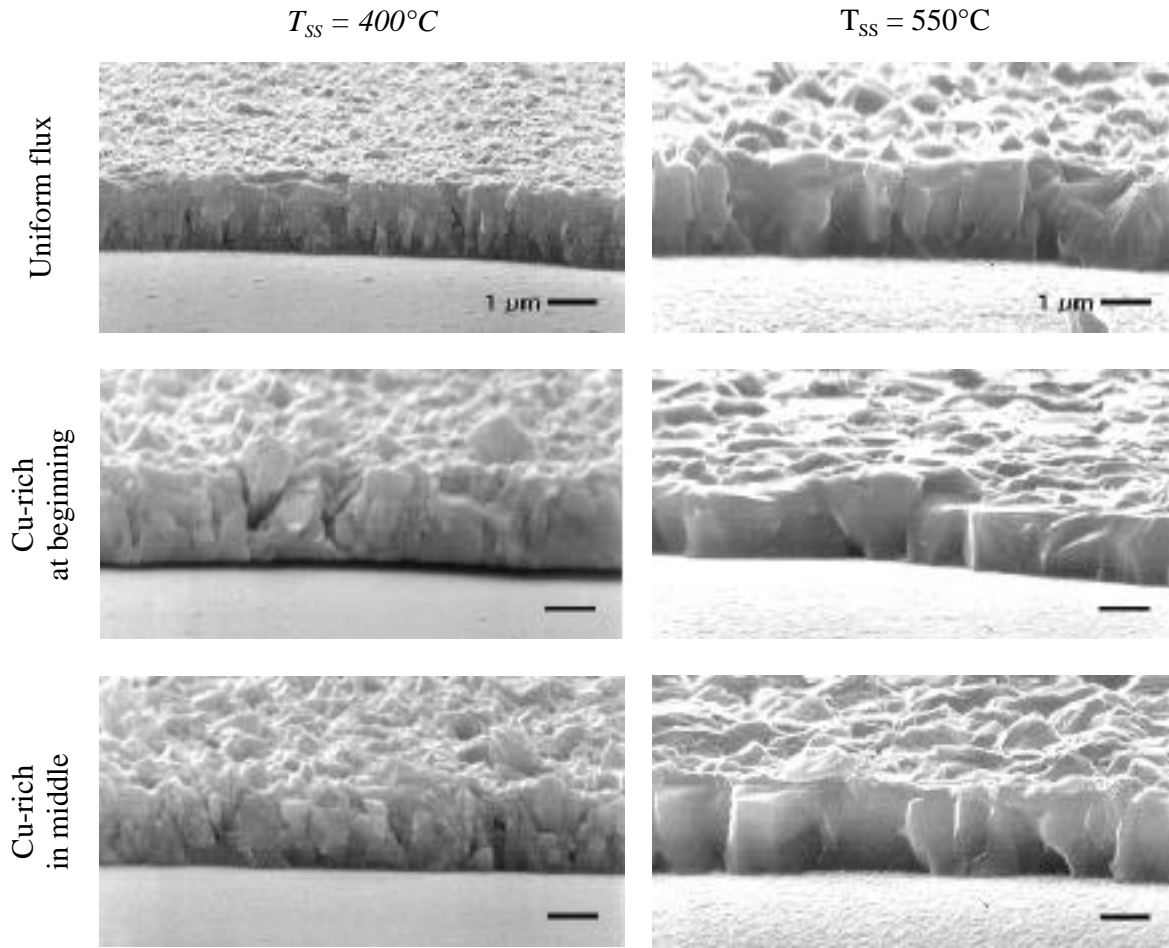


Fig. 2. Cross-sectional SEM micrographs of Cu(InGa)Se_2 films deposited with different flux profiles and T_{SS} .

These distributions are shown in Fig. 5 for the 6 different cases above. The number of grains in the $300 \mu\text{m}^2$ total sampling area, A and σ , are listed in Table 1. At 400°C , there is no significant difference in the distribution of lateral grain size at the surface. At 550°C , on the other hand, the mean area is smaller with the uniform flux process than for either Cu-rich process.

AES depth profiles were used to determine the compositional uniformity through the thickness of the films deposited at $T_{SS}=400^\circ\text{C}$. The films deposited with the three flux profiles showed uniform distribution of the Cu, In, and Ga through all the films with no compositional gradients despite the Cu flux gradient. In addition, we previously showed that the amount of Na which diffused in the films from the soda lime glass substrate is comparable for films deposited at 400

or 550°C with a flux profile Cu-rich at the beginning [3]. Finally, XRD measurements did not show any significant difference in the film orientation for different processes or temperatures. All the films had nearly random orientation, as has been found for films deposited on (110) oriented Mo films [6].

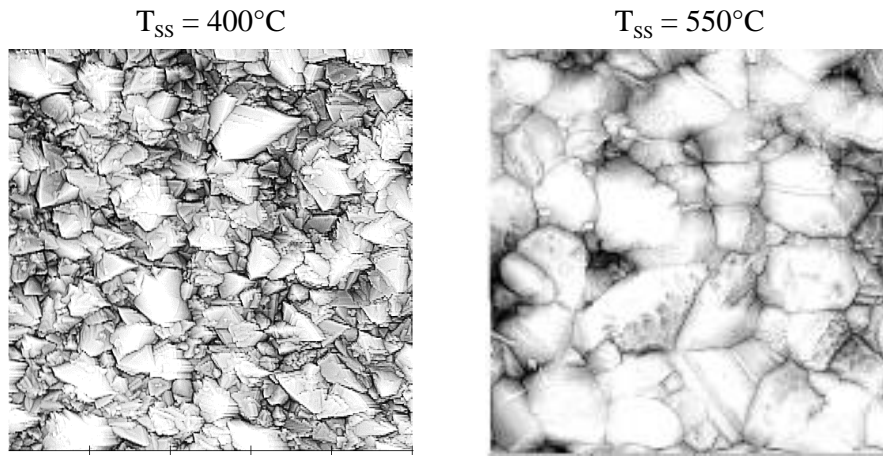


Fig. 3. AFM images of the top surface of films deposited with a Cu-rich flux at the beginning of the deposition. Each figure shows a 10 μm x 10 μm area.

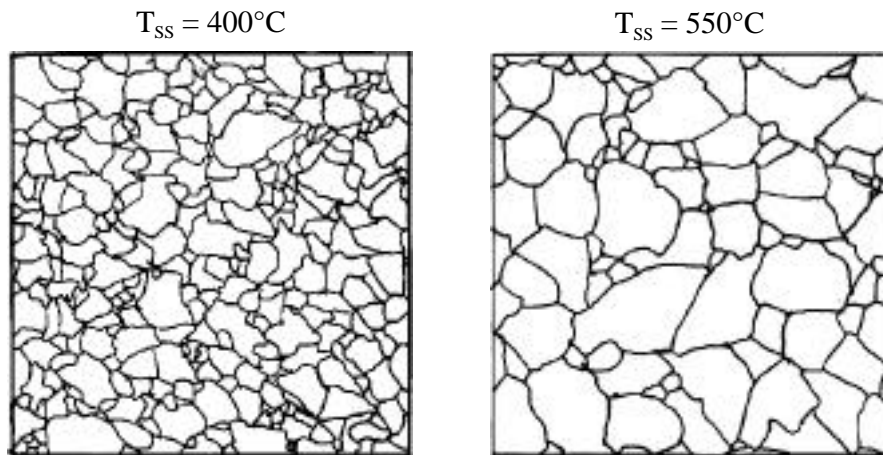


Fig. 4. Grain boundary maps created from the AFM images in Fig. 3.

Table 1
Number of grains in 300 μm^2 area and mean grain areas.

| Process | $T_{ss} = 400^\circ\text{C}$ | | | $T_{ss} = 550^\circ\text{C}$ | | |
|----------------------|------------------------------|-------------------------|--------------------------|------------------------------|-------------------------|--------------------------|
| | # of grains | A (μm^2) | ($\ln(\mu\text{m}^2)$) | # of grains | A (μm^2) | ($\ln(\mu\text{m}^2)$) |
| Uniform | 973 | 0.074 | 1.2 | 510 | 0.38 | 1.1 |
| Cu-rich in beginning | 952 | 0.080 | 1.1 | 316 | 0.54 | 1.5 |
| Cu-rich in middle | 984 | 0.066 | 1.1 | 325 | 0.57 | 1.2 |

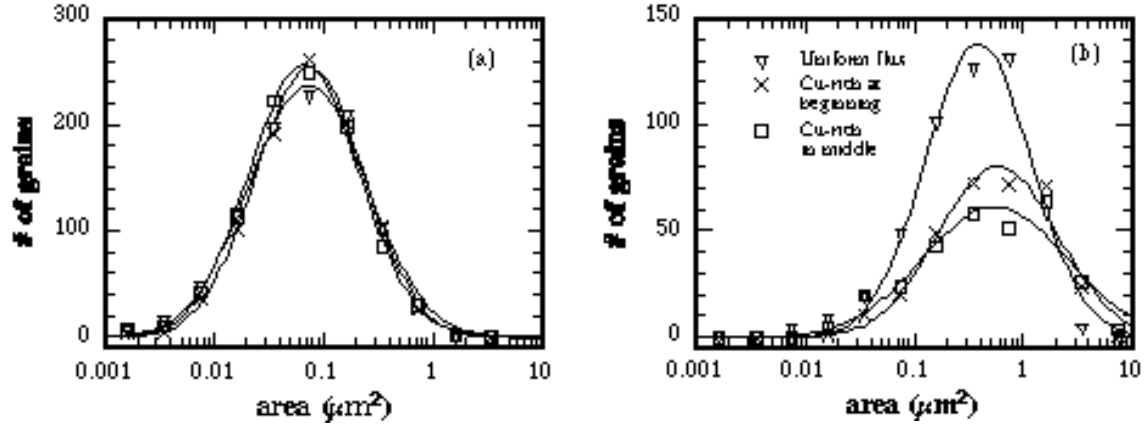


Fig. 5. Grain sizes showing log-normal distributions for films deposited at (a) 400°C and (b) 550°C.

Device results

The device performance for the best cells achieved with each process and temperature are summarized in Table 2. With $T_{SS} = 400^\circ\text{C}$, the Cu-rich flux, either in the beginning or the middle of the deposition, gives better device efficiency than the uniform flux. However, at 550°C there is no significant difference in the three processes. In repeated depositions the uniform process seems to be more reproducible in terms of producing high efficiency devices.

Table 2
Device performance with each process and temperature

| T_{SS} (°C) | Process | V_{oc} (V) | J_{sc} (mA/cm ²) | FF (%) | (%) |
|------------------|----------------------|-----------------|-----------------------------------|-----------|------|
| 400 | Uniform flux | 0.56 | 29 | 69 | 11.3 |
| | Cu-rich at beginning | 0.59 | 33 | 71 | 13.7 |
| | Cu-rich in middle | 0.60 | 33 | 71 | 13.8 |
| 550 | Uniform flux | 0.65 | 33 | 74 | 15.9 |
| | Cu-rich at beginning | 0.65 | 32 | 76 | 16.0 |
| | Cu-rich in middle | 0.65 | 32 | 75 | 15.5 |

The J-V curves under illumination and in the dark are shown in Fig. 6(a) for the two devices with the Cu-rich flux in the beginning of the deposition. The most significant difference is the increased voltage with higher T_{SS} . This cannot be attributed to the bandgap of the Cu(InGa)Se₂ absorber layer since the composition is the same and all films are compositionally uniform. As an aside, the J-V curves for all the 400°C samples show hysteresis between up and down traces where the data is measured with first increasing, then decreasing, voltage using a sweep time of ~ 1 min. This is more clearly seen in Fig. 6(b) where current is plotted on a logarithmic scale.

Finally, a 120 nm thick MgF₂ anti-reflection layer was deposited on the best cells above. This yielded cells with $\eta = 16.4\%$ for $T_{SS} = 550^\circ\text{C}$ and 14.1% with 400°C.

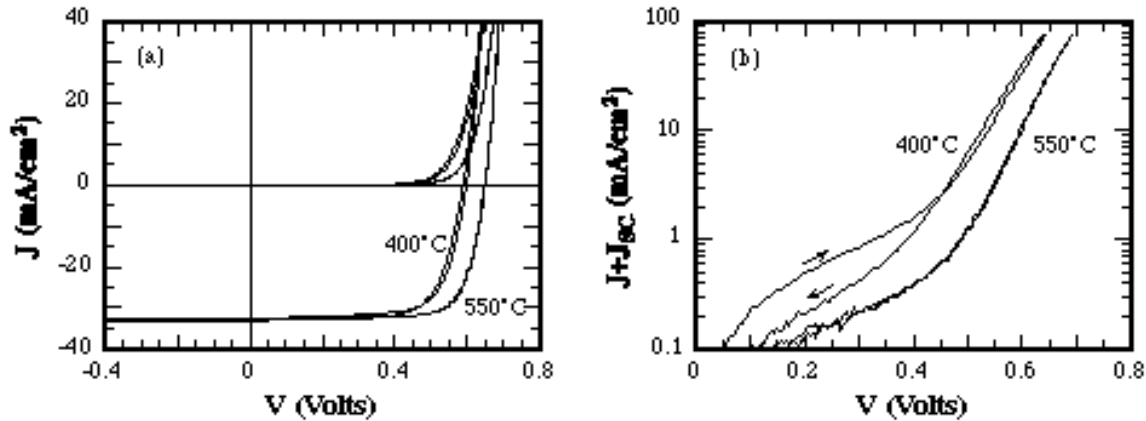


Fig. 6. J-V curves for devices with Cu(InGa)Se₂ deposited with a Cu-rich flux in the beginning. In (b) $J+J_{sc}$ is plotted for only the curve measured under illumination.

Conclusions

The device results with $T_{ss} = 400$ °C show that a Cu-rich growth step during the Cu(InGa)Se₂ deposition is needed to obtain the best device performance. However, the film and device results are the same whether the Cu-rich growth occurs during the initial nucleation or later in the process. This indicates tolerance to different process sequences which allows flexibility in deposition process design.

The larger grain films grown at 550°C give better performance than the smaller grain films at 400°C. But, with a given substrate temperature, there is no simple correlation between grain size and device performance. At the lower temperature, the improved cell results with Cu-rich growth cannot be explained by increased lateral grain size at the surface. Conversely, at the higher temperature, the increased grain size with the Cu-rich growth does not provide improved device performance.

In summary, the effects of T_{ss} on grain size and device performance have been investigated for Cu(InGa)Se₂ films deposited by elemental evaporation. At $T_{ss} = 550$ °C, which has yielded the highest efficiency devices, the device performance is insensitive to the use of Cu-rich growth. A simple process with constant fluxes throughout the deposition gives as high a device efficiency as processes incorporating graded fluxes to give Cu-rich growth. At 400°C, the uniform process gives more columnar grains but the same lateral grain size as the graded, Cu-rich processes. However, the best devices result from Cu-rich growth, although not necessarily during the initial film nucleation.

Acknowledgments

The authors would like to thank Erten Eser and Michael Engelmann for helpful discussions, Thomas Hughes-Lampros and Kevin Hart for depositions and device fabrication, and Alice Mason of NREL for Auger measurements. This work was funded by NREL under subcontract #ZAK-8-17619-33.

References

- [1] W. S. Chen, J.M. Stewart, W.E. Devaney, R.A. Mickelsen and B.J. Stanbery, Proc. Of 23rd IEEE Photovoltaic Specialists Conf., 1993, pp. 422-425.
- [2] R. Klenk, T. Walter, H.W. Schock and D. Cahen, *Advanced Material* **5**, 1993, p. 115.
- [3] W.N. Shafarman, R.W. Birkmire, S. Marsillac, M. Marudachalam, N. Orbey and TWF Russell, Proc. Of 26th IEEE Photovoltaic Specialists Conf., 1997, pp. 331-334.
- [4] W.N. Shafarman, R. Klenk, and B.E. McCandless, *J. Appl. Phys.* **79**(9), 1996, p. 7324.
- [5] K. Kurzydowski and B. Ralph, CRC Press, Boca Raton, FL, CRC Series in Mat. Sci. & Tech., 1995.
- [6] W. N. Shafarman, R.W. Birkmire, M. Marudachalam, B.E. McCandless and J.M. Schultz, NREL/SNL Photovoltaics Program Review, Lakewood, CO, 1996, pp. 123-131.